IEEE Access
Multidisciplinary | Rapid Review | Open Access Journal

Received April 15, 2020, accepted May 1, 2020, date of publication May 6, 2020, date of current version May 20, 2020.

Digital Object Identifier 10.1109/ACCESS.2020.2992635

Disturbance Attenuation for Surface-Mounted PMSM Drives Using Nonlinear Disturbance Observer-Based Sliding Mode Control

ANH TUAN NGUYEN, BILAL ABDUL BASIT, HAN HO CHOI, (Member, IEEE), AND JIN-WOO JUNG, (Member, IEEE)
Division of Electronics and Electrical Engineering, Dongguk University, Seoul 04620, South Korea

Corresponding author: Jin-Woo Jung (jinwjung@dongguk.edu)

This work was supported by the Basic Science Research Program through the National Research Foundation of Korea (NRF) funded by the Ministry of Education under Grant 2018R1D1A1B07046873.

ABSTRACT This paper proposes a nonlinear disturbance observer (NDO)-based sliding mode speed controller (SMSC) to guarantee the superior control performance in terms of robustness, fast transient response, and small steady-state error for a surface-mounted permanent magnet synchronous motor (SPMSM) drive. Generally, the control performance of the SPMSM drives can be degraded by disturbances, so an NDO with a proper disturbance rejection capability is proposed to appropriately improve the tracking performance of the SMSC designed for the SPMSM drives. Unlike the linear disturbance observers (LDOs), the proposed NDO can efficiently estimate the lumped disturbance such as uncertainties parameters and unmodeled dynamics by using the nonlinear design function. The proposed NDO rejects the complex disturbances as well as self-regulates the observer gains to increase the convergence rate. The feasibility of the proposed NDO-based SMSC is verified by using a MATLAB/Simulink software program and a prototype SPMSM drive system with a TI TMS320F28335 digital signal processor (DSP). The comparative results with a conventional LDO-based SMSC are analyzed under load torque disturbances and model uncertainties to prove the excellent performance of the proposed NDO-based SMSC.

INDEX TERMS Nonlinear disturbance observer (NDO), sliding mode speed controller (SMSC), surface-mounted permanent magnet synchronous motor (SPMSM).

I. INTRODUCTION

Currently, the permanent magnet synchronous motors (PMSMs) occupy a major proportion when compared with other motors in the contemporary drive applications (e.g., electric vehicles, servo drives, industrial processes, etc.) because of their advanced features such as high efficiency, high power density, wide range operation, simple structure, and compact size [1]–[4]. In controlling the PMSMs, the disturbance (e.g., load torque disturbance, and parameter uncertainties) is one of the factors that degrades the control performance of the drive system (e.g., transient response, robustness, etc.), so it is needed to be rejected [5]–[7]. However, it is not an easy task to properly reject the disturbances in industrial applications because these disturbances are mostly not measurable in industrial motor drives. Thus, an appropriate disturbance observer (DO) is required, which can precisely estimate the disturbances.

In recent decades, various DOs in the control schemes are designed to attenuate the disturbances and uncertainties in the ac motor drives [8]. In general, the DOs can be classified as such: linear disturbance observer (LDO) [9]–[12] and nonlinear disturbance observer (NDO) [13], [14]. In [9] and [10], the disturbance compensator is designed relying on the frequency-domain for the PMSM drives. These LDOs are designed by using the transfer function techniques to find an appropriate filter that compensates for the feedforward part of the controller in the PMSM drives. However, the stability of the drive system is not easy to be assured and its implementation is limited in the trial and error technique. Also, in the DOs mentioned above, the low-pass filter (LPF) should be used to acquire the evaluated parameters, which cause the phase delay and amplitude attenuation, then decrease the estimation accuracy. In [11] and [12], the

The associate editor coordinating the review of this manuscript and approving it for publication was Atif Iqbal.

This work is licensed under a Creative Commons Attribution 4.0 License. For more information, see https://creativecommons.org/licenses/by/4.0/

state-space-based methods are used for the linear dynamic systems or the linearizable nonlinear systems. In [11], an active disturbance rejection control (ADRC) scheme is adopted to perform the angular velocity trajectory tracking mission by using the high-gain generalized proportional integral observer (GPIO) for the PMSM drives. In [12], a linear extended state observer (LESO) used as an elementary part of the ADRC method is presented for adapting to the robust backstepping tracking controller in the PMSM drives. Although the LDO methods in [11] and [12] can achieve good performance, both of them have poor robustness against the variations in the electrical parameters of the SPMSM. In [13], the NDO is investigated to compensate for the offsets caused by the external load torque and parametric uncertainties. In [14], an adaptive DO scheme using the back-EMF estimation and the dynamic internal model is presented for the current controller in the PMSM drive. However, the modeling inaccuracy and disturbances included in the lumped disturbances are not considered.

Some control methods combined with the NDO for PMSM drive are presented in the previous studies, such as model predictive control (MPC) [15], fuzzy control [16], [17], adaptive control [18], [19], and sliding mode control (SMC) [20]–[25]. In [15], the cogging torque disturbance is estimated by the DO and look-up table combined with a finite control set (FCS) MPC scheme at low speed. However, the disturbances with the complex forms (e.g., parameter uncertainties, other unmodeled dynamics, etc.) in the real-time PMSM drives are not considered. In [16] and [17], the DOs are combined with the fuzzy controller. However, it has a computational burden in the calculation of digital signal processor (DSP) when regarding the involved disturbances. In [18], a robust adaptive torque observer is incorporated into a hybrid-type variable structure for instantaneous torque control. However, it does not show the efficacy of the disturbance rejection of the whole drive system. In [19], the DO is designed to support a robust adaptive controller by compensating for parameter uncertainties and input saturation. However, the performance is not compared fairly to another common approach. In [20] and [21], the DOs are designed to provide the compensation terms for the sliding mode controller. However, the factors of the complicated disturbances are not solved completely to render the better performance. In [22], the NDO is presented to compensate for the lumped disturbances. However, the method that chooses the observer gain matrix is vague. In [23], an adaptive nonsingular terminal sliding mode control based on the DO is introduced by using an improved exponential reaching law to shorten the settling time. In [24], another nonsingular terminal sliding mode control based on the DO is presented to eliminate the modeled disturbance and compensate for the norm-bounded disturbance. In [25], an adaptive sliding mode current control with a sliding mode DO for PMSM is designed to improve the performance of the current loop in terms of the transient speed response, zero tracking error, and robustness. However, these methods [23]–[25] have the complex algorithms despite good control performance. Thus, the NDO is required to achieve the improved performance by estimating the disturbances and rejecting these disturbances in the PMSM drives.

This paper proposes an NDO-based sliding mode speed controller (SMSC) to ensure good control performance such as robustness against parameter variations and external disturbances, fast transient response, and small steady-state error (SSE) for an SPMSM drive. In general, the disturbances can significantly degrade the overall control performance of the system in the practical SPMSM drives. Thus, an NDO with a proper disturbance rejection capability is proposed to properly enhance the speed tracking performance of the designed SMSC for the SPMSM drives. Unlike the LDOs, the proposed NDO using the nonlinear design function can effectively estimate the lumped disturbances in terms of uncertainties parameters and unmodeled dynamics. The proposed NDO rejects the complicated disturbances as well as self-tunes the observer gains to increase the convergence rate. Finally, the original performance of the SMC is preserved since the proposed NDO plays a supplementary role for the controller, whereas the NDO does not cause negative effects on the system in case of no uncertainties. The overall performance of the SPMSM control system (e.g., robustness, fast transient response, and small steady-state error) is remarkably enhanced by using the proposed NDO-based SMSC. To validate the efficacy of the proposed scheme, the comparative studies with a conventional LDO-based SMSC are carried out through a MATLAB/Simulink software package and a prototype SPMSM drive system with a TI TMS320F28335 DSP under load torque disturbances and model parameter variations.

II. DYNAMIC MODEL OF AN SPMSM WITH LUMPED DISTURBANCES

The dynamic model of an SPMSM can be described in the synchronously rotating d-q reference frame as follows [3]:

$$\begin{cases} \dot{\omega} = g_1 i_{qs} - g_2 \omega - g_3 T_L + \delta_\omega \\ \dot{i}_{qs} = -g_4 i_{qs} - g_5 \omega + g_6 v_{qs} - \omega i_{ds} + \delta_q \\ \dot{i}_{ds} = -g_4 i_{ds} + g_6 v_{ds} + \omega i_{qs} + \delta_d \end{cases} \tag{1}$$

where $g_1 = 3p^2\phi_f/8J$, $g_2 = B/J$, $g_3 = p/2J$, $g_4 = R_s/L_s$, $g_5 = \phi_f/L_s$, $g_6 = 1/L_s$, ω is the electrical rotor speed considered as the controlled output, i_{qs} and i_{ds} are the q-axis and d-axis stator currents, T_L is the load torque disturbance, v_{qs} and v_{ds} are the q-axis and d-axis stator voltages considered as the control inputs, ϕ_f is the magnetic flux linkage, J is the rotor moment of inertia, B is the viscous friction coefficient, p is the number of poles, L_s is the stator inductance, R_s is the stator resistance, and δ_ω, δ_q, and δ_d denote the unmodeled dynamics [26]. The uncertainties of the parameters (g_1,..., g_6) are denoted as Δg_1,..., Δg_6, respectively.

From (1), the dynamic model considering the parameter uncertainties is represented as follows:

$$\begin{cases} \dot{\omega} = g_1 i_{qs} - g_2 \omega + d_\omega \\ \dot{i}_{qs} = -g_4 i_{qs} - g_5 \omega + g_6 v_{qs} - \omega i_{ds} + d_q \\ \dot{i}_{ds} = -g_4 i_{ds} + g_6 v_{ds} + \omega i_{qs} + d_d \end{cases} \tag{2}$$

where d_ω, d_q, and d_d denote the lumped disturbances as

$$\begin{aligned} d_\omega &= \Delta g_1 i_{qs} - \Delta g_2 \omega - (g_3 + \Delta g_3) T_L + \delta_\omega \\ d_q &= -\Delta g_4 i_{qs} - \Delta g_5 \omega + \Delta g_6 v_{qs} + \delta_q \\ d_d &= -\Delta g_4 i_{ds} + \Delta g_6 v_{ds} + \delta_d. \end{aligned} \tag{3}$$

It is supposed that the above lumped disturbances are bounded with a certain varying rate (i.e., $|d_i(t)| < \eta_i$ with $\eta_i > 0$, $i = \omega$, q, and d). Also, for simplicity, the following assumptions are set to design the proposed NDO-based SMSC scheme.

Assumptions: 1) ω, i_{qs}, and i_{ds} are measurable; 2) T_L is unknown and varies slowly during a small sampling period.

III. NDO DESIGN AND STABILITY ANALYSIS

This section designs an NDO to precisely estimate the lumped disturbances defined in (3). Its stability is also analyzed by using a Lyapunov function.

A. NDO DESIGN

Unlike the dynamic models of the PMSMs applied in [1], [3], this paper uses the lumped disturbances which cover all uncertainties of the parameters (i.e., $\Delta g_1, \ldots, \Delta g_6$) and unmodeled dynamics (i.e., δ_ω, δ_q, and δ_d) in the mechanical dynamics (i.e., ω) and electrical dynamics (i.e., i_{qs} and i_{ds}). It is noted that the load torque (T_L) is included in the lumped disturbance d_ω which can be rejected by the proposed SMSC to be presented in Section V. To simplify the dynamic model (2), the control inputs (v_{qs} and v_{ds}) are defined as

$$v_{qs} = u_{oq} + \omega i_{ds}/g_6, \quad v_{ds} = u_{od} - \omega i_{qs}/g_6 \tag{4}$$

where u_{oq} and u_{od} are considered as the control input of the modified dynamic model used for designing the NDO below.

By substituting (4) into (2), the following dynamic model can be achieved to design the NDO:

$$\dot{x}_o = \mathbf{A}_o x_o + \mathbf{B}_o u_o + d \tag{5}$$

where $x_o = [\omega, i_{qs}, i_{ds}]^T$, $u_o = [u_{oq}, u_{od}]^T$, $d = [d_\omega, d_q, d_d]^T$,

$$\mathbf{A}_o = \begin{bmatrix} -g_2 & g_1 & 0 \\ -g_5 & -g_4 & 0 \\ 0 & 0 & -g_4 \end{bmatrix}, \text{ and } \mathbf{B}_o = \begin{bmatrix} 0 & 0 \\ g_6 & 0 \\ 0 & g_6 \end{bmatrix}.$$

The disturbances term in the dynamic model (5) can be distinctively gathered and rewritten as

$$d = \dot{x}_o - \mathbf{A}_o x_o - \mathbf{B}_o u_o. \tag{6}$$

Hence, an NDO [26]–[28] is designed as

$$\begin{aligned} \dot{z} &= -L(x_o) z - L(x_o)[p(x_o) + \mathbf{A}_o x_o + \mathbf{B}_o u_o], \\ \hat{d} &= z + p(x_o), \end{aligned} \tag{7}$$

where $z \in R^3$ is an internal state variable of the nonlinear observer, $\hat{d}$ is an estimate of d, $p(x_o)$ is a function vector to be designed, and $L(x_o)$ is an observer gain matrix defined as $L(x_o) = \partial p(x_o)/\partial x_o$ [26], [28].

In this paper, the disturbances are assumed to change slowly during a small sampling time (T_s) in ac motor drives, so the first-order derivative of lumped disturbances is considered to be zero. Then, the disturbance estimation error can be established as

$$\tilde{d} = d - \hat{d}. \tag{8}$$

The NDO (7) can exponentially track the constant disturbance if the observer gain matrix $L(x_o)$ is chosen such that [26]–[28]

$$\dot{\tilde{d}} = -L(x_o)\tilde{d} \tag{9}$$

which is globally exponentially stable regardless of for all $x_o \in R^3$. In [26]–[28], it is difficult to choose the observer gain matrix $L(x_o)$ that efficiently compensates for the disturbances appearing in the SPMSM drives owing to the linear design function $p(x_o)$. Moreover, the disturbance observer possesses a slower convergence rate because of the fixed gains of $L(x_o)$ at some critical scenarios such as load torque step-change [28]. Given the nonlinear design function $p(x_o) \in R^3$ and the observer gain $L(x_o) \in R^{3\times 3}$, $L(x_o)$ is selected as the gradient of the function vector $p(x_o)$ with respect to $x_o = [\omega, i_{qs}, i_{ds}]^T$ [27]. Thus, the nonlinear design function $p(x_o)$ is proposed as

$$p(x_o) = \begin{bmatrix} m_1\omega + m_2\omega^3 & m_3 i_{qs} + m_4 i_{qs}^3 & m_5 i_{ds} + m_6 i_{ds}^3 \end{bmatrix}^T \tag{10}$$

where $m_i > 0\,(i = 1, 2, \ldots, 6)$ are constant parameters. In [29] and [30], the conventional LDOs using the linear design function $p(x_o)$ estimate the disturbances with a slow convergence rate. In addition, the conventional LDO in [30] does not mention the lumped disturbances that require an appropriate estimation. Unlike the conventional LDOs, the proposed NDO uses the nonlinear design function $p(x_o)$ including the first-order and third-order state variables. By obtaining the time derivative of the nonlinear design function (10), the nonlinear observer gain matrix $L(x_o)$ can be represented as

$$\begin{aligned} L(x_o) &= \partial p(x_o)/\partial x_o \\ &= \begin{bmatrix} m_1 + 3m_2\omega^2 & 0 & 0 \\ 0 & m_3 + 3m_4 i_{qs}^2 & 0 \\ 0 & 0 & m_5 + 3m_6 i_{ds}^2 \end{bmatrix}. \end{aligned} \tag{11}$$

Note that the observer matrix gain $L(x_o)$ is selected to satisfy the condition of the globally exponential stability of the disturbance estimation errors in (9). It is clear that the higher matrix gain $L(x_o)$ will force the exponential convergence rate of these disturbance estimation errors to be faster [31]. Thus, it can be known in (11) that the nonlinear gain matrix $L(x_o)$ can enable the proposed NDO to increase the convergence

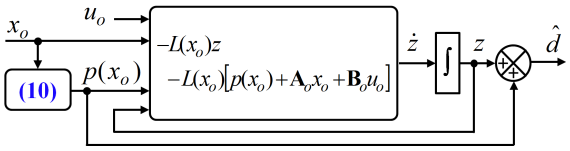

FIGURE 1. Block diagram of the proposed NDO.

rate by using the high gains updated online with the square of equivalent state variable of each eigenvalue. Fig. 1 displays the block diagram of the proposed NDO.

B. STABILITY ANALYSIS

This subsection can briefly analyze the convergence and stability of the proposed NDO. Let the Lyapunov function be given by $V = \tilde{d}^T\tilde{d}$. Then its time derivative along (9) is reduced to $\dot{V} = -2\tilde{d}^T L(x)\tilde{d} \leq -2m_0\tilde{d}^T\tilde{d} \leq 0$ where m_0 is the minimum constant among m_1, m_3, and m_5. This implies that $V(t) \leq V(0)e^{-2m_0t}$or equivalently $||\tilde{d}(t)|| \leq ||\tilde{d}(0)||e^{-m_0t}$, i.e., the disturbance estimation error converges exponentially to zero. This implies that if the nonlinear design function $p(x_o)$ is chosen as (10), the proposed NDO (7) is exponentially stable.

Remark 1: In this section, an NDO for the SPMSM drive is proposed to increase the disturbance rejection capability. The disturbance observers reported in the previous references [20], [21] mainly estimate the external load torque disturbances. Meanwhile, the proposed NDO (7) can efficiently estimate the lumped disturbance terms. In [23], a DO is presented to evaluate the lumped disturbances. However, this DO is designed to estimate only the lumped disturbance in the mechanical dynamics for the speed loop of the PMSM with the cascaded control structure. Whereas, the proposed NDO (7) can observe the lumped disturbances in both the mechanical dynamics and electrical dynamics terms (i.e., d_ω, d_q, and d_d). Additionally, unlike the DO presented in [22], [24], the nonlinear observer gain matrix $L(x_o)$ of the proposed NDO (7) is defined with the presence of the state feedback updated online in the entry values, while the observer gain in [22], [24] includes the fixed values. Therefore, the proposed NDO can give the precisely estimated results with a faster convergence rate compared to the DO presented in [22], [24].

Remark 2: The parameters in the observer matrix gain $L(x_o)$ can be chosen by using a trial-and-error method in accordance with the following parameter tuning guideline:

1) First, select an small value of $m_1,\ldots, m_6$ ($m_i > 0$ for $i = 1, 2,\ldots, 6$) to intensively study the simulation results. It should be noted that the lumped disturbance in the mechanical dynamics (d_ω) is exactly estimated with the properly selected parameters (m_1 and m_2). Also, the lumped disturbance in the electrical dynamics (d_q and d_d) is precisely observed with the appropriately selected parameters (m_3, m_4, m_5, and m_6).

2) Increase the parameters m_1 and m_2 at a low speed condition to get a high gain for well estimating the load torque change. However, in case of a high speed, the parameters m_1 and m_2 can be reduced to a bounded value to guarantee the good speed tracking.

3) Select the parameters m_3, m_4, m_5, and m_6 based on the degree of motor parameter variations. Although the parameter variations are practically unknown, the degree of parameter variations can be evaluated via the speed and load torque. With a high speed and high load torque of the motor, the degree of parameter variations is increased proportionately. In this condition, the high values for the parameters m_3, m_4, m_5, and m_6 are essential.

IV. NDO-BASED SMSC DESIGN AND STABILITY ANALYSIS

This section designs the NDO-based SMSC to optimize the estimation capability of the proposed NDO (7) investigated in Section III.

A. SMSC DESIGN

To develop the proposed controller, the nonlinear model (2) of the SPMSM needs to be changed to a proper error dynamic model. Thus, the speed error and q-axis current error can be defined as

$$\tilde{\omega} = \omega - \omega_d, \quad \tilde{i}_{qs} = i_{qs} - i_{qsd} \tag{12}$$

where ω_d is the desired rotor speed and i_{qsd} is the q-axis current reference that can be defined as

$$i_{qsd} = \frac{(g_2\omega_d + \dot{\omega}_d - d_\omega)}{g_1}. \tag{13}$$

In this paper, it is noted that the i_{qsd} should include the lumped disturbance in the mechanical dynamics as defined in (13) due to the intrinsic torque component current in the indirect vector control [25], [29]. Meanwhile, the d-axis current reference (i_{dsd}) is set to zero owing to the rotor non-saliency of an SPMSM. From (2), (12), and (13), the error dynamic model considering the parameter uncertainties is represented as follows:

$$\begin{cases} \dot{\tilde{\omega}} = g_1\tilde{i}_{qs} - g_2\tilde{\omega} \\ \dot{\tilde{i}}_{qs} = -g_4\tilde{i}_{qs} - g_5\tilde{\omega} + g_6v_{qs} - \omega i_{ds} - g_4i_{qsd} \\ \qquad\quad - g_5\omega_d - \dfrac{g_2\dot{\omega}_d + \ddot{\omega}_d}{g_1} + d_q \\ \dot{i}_{ds} = -g_4i_{ds} + g_6v_{ds} + \omega i_{qs} + d_d, \end{cases} \tag{14}$$

where the derivative of the lumped disturbance is neglected due to the supposition of a bounded varying rate as mentioned in Section II (i.e., $\dot{\hat{d}}_\omega = 0$).

The control inputs (v_{qs} and v_{ds}) are decomposed into the feedforward and feedback control terms to handle the remaining nonlinearities terms in (14) as

$$v_{qs} = u_{qc} + u_{qs}, \quad v_{ds} = u_{dc} + u_{ds} \tag{15}$$

where

$$\begin{aligned} u_{qc} &= \frac{1}{g_6}\left(\omega i_{ds} + g_4i_{qsd} + g_5\omega_d + \frac{g_2\dot{\omega}_d + \ddot{\omega}_d}{g_1}\right) \\ u_{dc} &= -\frac{\omega i_{qs}}{g_6} \end{aligned} \tag{16}$$

are considered as the feedforward components which compensate for the nonlinear dynamics of the SPMSM drive, whereas u_{qs} and u_{ds} are considered as the feedback components that stabilize the error dynamics. It is noted that u_{qs} and u_{ds} can be also considered as the new control inputs after transformed with (15). By substituting (15) into (14), the following error dynamic model can be achieved:

$$\dot{x} = \mathbf{A}x + \mathbf{B}u + d_c, \tag{17}$$

where $x = [\widetilde{\omega}, \widetilde{i}_{qs}, i_{ds}]^T$, $u = [u_{qs}, u_{ds}]^T$, $d_c = [0, d_q, d_d]^T$,

$$\mathbf{A} = \begin{bmatrix} -g_2 & g_1 & 0 \\ -g_5 & -g_4 & 0 \\ 0 & 0 & -g_4 \end{bmatrix}, \text{ and } \mathbf{B} = \begin{bmatrix} 0 & 0 \\ g_6 & 0 \\ 0 & g_6 \end{bmatrix}.$$

It is noted that the error dynamic model (17) linearizes the dynamic model (1) by gathering the lumped disturbances that comprise the external load torque, parameter uncertainties, and unmodeled dynamics. Additionally, the linearized model (17) can assist the stability proof of the proposed control scheme. Thus, the estimation of these lumped disturbances using the NDO in the previous section can improve the robust performance of the proposed scheme.

Generally, the SMC system design can be separated into two independent steps [16], [32], [33]. In the first step, a sliding surface for the sliding mode is designed. The second step is to choose a switching feedback control law that assures the reachability condition in the presence of uncertainties.

Let us define a new variable q as

$$q = g_1\widetilde{i}_{qs} - g_2\widetilde{\omega}. \tag{18}$$

Then, the error dynamic model (17) can be rewritten as

$$\begin{cases} \dot{\widetilde{\omega}} = q \\ \dot{q} = -(g_1g_5 + g_2g_4)\widetilde{\omega} - (g_2 + g_4)q + g_1g_6u_{qs} + g_1d_q \\ \dot{i}_{ds} = -g_4i_{ds} + g_6u_{ds} + d_d. \end{cases} \tag{19}$$

The sliding surface can be designed as

$$\sigma = \begin{bmatrix} \sigma_q \\ \sigma_d \end{bmatrix} = \begin{bmatrix} c\widetilde{\omega} + \dot{\widetilde{\omega}} \\ i_{ds} \end{bmatrix} = \begin{bmatrix} c\widetilde{\omega} + q \\ i_{ds} \end{bmatrix} \tag{20}$$

where c satisfies the Hurwitz condition [27], $c > 0$.

The time derivative of the sliding mode function vector can be expressed as follows:

$$\begin{bmatrix} \dot{\sigma}_q \\ \dot{\sigma}_d \end{bmatrix} = \begin{bmatrix} -(g_1g_5 + g_2g_4)\widetilde{\omega} - (g_2 + g_4 - c)q \\ \qquad + g_1g_6u_{qs} + g_1d_q \\ -g_4i_{ds} + g_6u_{ds} + d_d \end{bmatrix}. \tag{21}$$

By adopting the reaching law with a constant rate for the sliding mode function, the control inputs (u_{qs}, u_{ds}) of the error dynamic model (19) can be obtained as the following sliding mode controller:

$$\begin{aligned} u_{qs} &= \frac{1}{g_1g_6}\begin{pmatrix} (g_1g_5 + g_2g_4)\widetilde{\omega} + (g_2 + g_4 - c)q \\ -g_1d_q - k_q\text{sgn}(\sigma_q) \end{pmatrix} \\ u_{ds} &= \frac{1}{g_6}\left(g_4i_{ds} - d_d - k_d\text{sgn}(\sigma_d)\right) \end{aligned} \tag{22}$$

where $k_q > 0$ and $k_d > 0$.

B. NDO-BASED SMSC DESIGN AND STABILITY ANALYSIS

It should be noted that the lumped disturbance d_ω is included in the q-axis current reference (13). By utilizing the estimated lumped disturbance in the mechanical dynamics (i.e., $\hat{d}_\omega$), the estimated q-axis current reference is rewritten as

$$\hat{i}_{qsd} = \frac{(g_2\omega_d + \dot{\omega}_d - \hat{d}_\omega)}{g_1}. \tag{23}$$

Also, by using the NDO (7) designed in Section III, the control inputs (22) of the error dynamic model (19) are rewritten as

$$\begin{aligned} u_{qs} &= \frac{1}{g_1g_6}\begin{pmatrix} (g_1g_5 + g_2g_4)\widetilde{\omega} + (g_2 + g_4 - c)q \\ -g_1\hat{d}_q - k_q\text{sgn}(\hat{\sigma}_q) \end{pmatrix} \\ u_{ds} &= \frac{1}{g_6}\left(g_4i_{ds} - \hat{d}_d - k_d\text{sgn}(\sigma_d)\right) \end{aligned} \tag{24}$$

where $\hat{\sigma}_q = c\widetilde{\omega} + \hat{q}$ and $\hat{q} = g_1(i_{qs} - \hat{i}_{qsd}) - g_2\widetilde{\omega}$. From (15) and (24), the control inputs (v_{qs}, v_{ds}) of the error dynamic model (14) are designed as

$$\begin{aligned} v_{qs} &= \frac{1}{g_1g_6}\begin{pmatrix} (g_1g_5 + g_2g_4)\widetilde{\omega} + (g_2 + g_4 - c)q + g_1\omega\, i_{ds} \\ \quad + g_1g_4\hat{i}_{qsd} + g_1g_5\omega_d + g_2\dot{\omega}_d + \ddot{\omega}_d \\ \quad - g_1\hat{d}_q - k_q\text{sgn}(\hat{\sigma}_q) \end{pmatrix} \\ v_{ds} &= \frac{1}{g_6}\left(g_4i_{ds} - \omega\, i_{qs} - \hat{d}_d - k_d\text{sgn}(\sigma_d)\right). \end{aligned} \tag{25}$$

Remark 3: Note that the control inputs (v_{qs} and v_{ds}) include the lumped disturbances estimated with more exact values based on the proposed NDO (7). This enhances the disturbance rejection capability of the whole control system. Also, the chattering issues caused by the last terms with high gains in (25) can be compensated for by the terms that consist of the estimated disturbances [5], [33]. To select the switching gains (k_q and k_d), it is essential to know the upper bounds of the parameter uncertainties. Additionally, the gains (k_q and k_d) are chosen based on the adaptation mechanism by considering the trade-off between the steady-state error and the chattering phenomenon [34]. Fig. 2 exhibits the block diagram of the proposed NDO-based SMSC.

Then, the stability analysis of an SMC system is classified into two stages. The first stage is to show the stability of the sliding mode dynamics, whereas the second stage is to verify the reachability condition. First, by setting $\sigma = \dot{\sigma} = 0$ and using the equivalent control method, it can be observed that the sliding mode dynamics limited to $\sigma = 0$ is given by

$$\dot{\widetilde{\omega}} = -c\widetilde{\omega}. \tag{26}$$

which is asymptotically stable if $c > 0$.

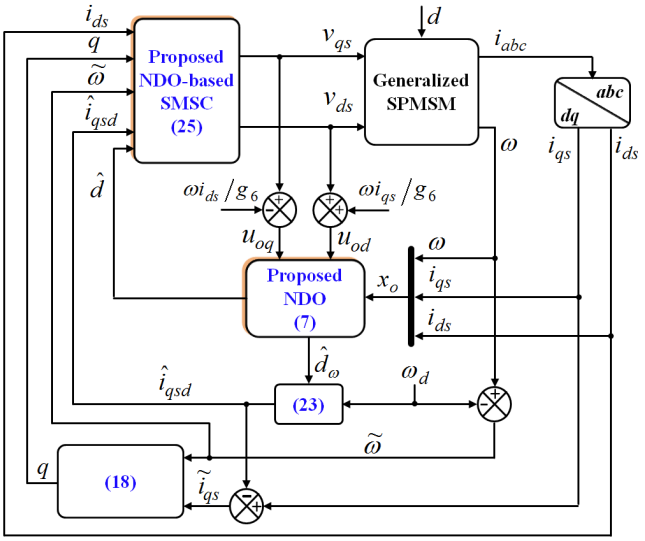

FIGURE 2. Block diagram of the proposed NDO-based SMSC.

Second, by using (19) and (20), it can be easily identified that the following reachability condition is satisfied for all nonzero σ:

$$\sigma^T \dot{\sigma} \leq 0. \tag{27}$$

Let us define the Lyapunov function as follows:

$$V = \frac{\sigma^2}{2}. \tag{28}$$

Then, the time derivative of $V(t)$ is achieved as

$$\dot{V}(t) = \sigma^T \dot{\sigma}. \tag{29}$$

From (19)–(22), the generalized dissipation function in (29) is written as

$$\begin{aligned} \dot{V}(t) &= -k_q \sigma_q \text{sgn}(\sigma_q) - k_d \sigma_d \text{sgn}(\sigma_d) \\ &= -k_q |\sigma_q| - k_d |\sigma_d| \leq 0 \end{aligned} \tag{30}$$

which shows that σ converges to zero. This proves the following: Suppose that the NDO (7) is asymptotically stable and there exist a sliding surface (20) and a feedback control law (24). Then, the proposed NDO-based SMSC (25) makes the state of the system (14) converge to zero. As mentioned in the literature [31], [32], [35], the separation principle can hold the stabilization of the proposed closed-loop system with the designed observer. It means that the stability of the NDO and the stability of the SMSC can be proven independently.

Remark 4: The proposed control law includes two terms: the feedforward compensation term (24) and the feedback stabilization term (15). The former term is proposed to compensate for the nonlinearities and lumped disturbances by using the proposed NDO, which helps the proposed controller be robust against parameter variations and uncertainties. The latter term is designed by the simplified adaptive sliding surface (20), which stabilizes the proposed controller to guarantee a good transient performance for the SPMSM drives. Additionally, the chattering problem appearing in the proposed NDO-based SMSC (25) is attenuated by the disturbance compensation terms derived from the proposed NDO (7). Thus, the proposed NDO yields not only the robust capability against the lumped disturbances but also the good tracking performance for the SPMSM control system.

TABLE 1. Nominal SPMSM parameters.

Parameter	Symbol	Value
Rated speed	ω_{Rated}	3000 r/min
Rated power	P_{Rated}	750 W
Rated load torque	$T_{L-Rated}$	2.4 N·m
Rated phase current	I_{Rated}	4.3 A
Stator resistance	R_s	0.43 Ω
Stator inductance	L_s	3.2×10^{-3} H
Number of poles	p	8
Magnet flux linkage	ϕ_f	0.085 V·s/rad
Equivalent rotor inertia	J	1.8×10^{-3} kg·m^2
Viscous friction coefficient	B	0.2×10^{-3} N·m·s/rad

Remark 5: The gains of the SMSC (25) can be selected based on the following parameter tuning guideline:

1) Choose an initial value c with a small value for the sliding surface (20) to meet the fast transient response requirements.

2) With the gains (k_q and k_d), too small values can lead to a slow transient response, whereas too large values can cause the chattering problem in the steady-state response. Thus, a small value of the gains (k_q and k_d) are more suitable for a steady-state operating condition because the transient response can be compensated by choosing the coefficient c.

As a result, the design procedure of the proposed NDO-based SMSC can be summarized as follows:

Step 1) Build the matrices $\mathbf{A}_o$ and $\mathbf{B}_o$ for the dynamic model (5).

Step 2) Measure ω, i_{qs}, and i_{ds} to create the state variable x_o of the nonlinear disturbance observer (7).

Step 3) Set the proper observer gain matrix $L(x_o)$ following (11) via extensive simulation studies.

Step 4) Establish the matrices**A** and **B** for the error dynamic model (17).

Step 5) Construct the control inputs (v_{qs} and v_{ds}) following the control law (25) after replacing the lumped disturbances (d_ω, d_q, d_d) with the estimated lumped disturbances ($\hat{d}_\omega$, $\hat{d}_q$, $\hat{d}_d$) and the q-axis current reference (i_{qsd}) with the estimated q-axis current reference ($\hat{i}_{qsd}$).

Step 6) Select the suitable coefficient c and switching gains (k_q and k_d) via extensive simulation studies.

V. COMPARATIVE VERIFICATION RESULTS

To evaluate the robust performance of the proposed NDO-based SMSC for the SPMSM drive, the simulations on a MATLAB/Simulink software and the experiments on a prototype SPMSM drive system are conducted with the nominal SPMSM parameters listed in Table 1.

Fig. 3 illustrates the overall experimental setup of a prototype test-bed SPMSM drive with a Texas Instruments (TI) TMS320F28335 DSP. In this test-bed, the SPMSM drive

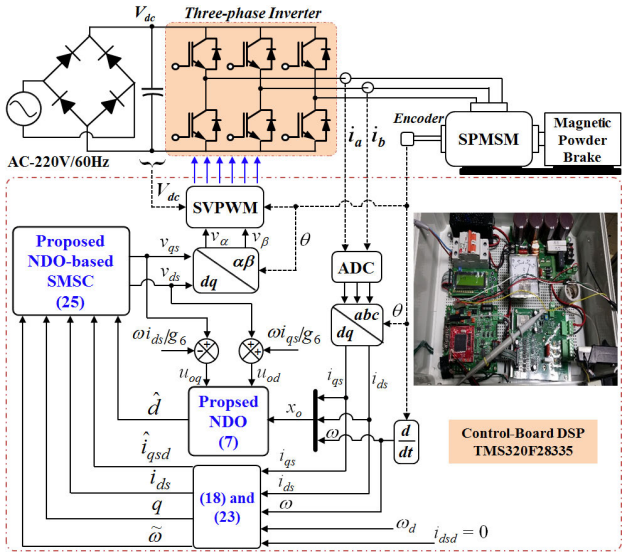

(a)

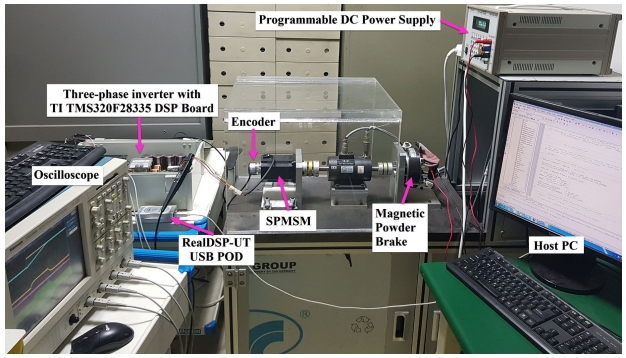

(b)

FIGURE 3. Experimental platform of a prototype test bed SPMSM drive with a TI TMS320F28335 DSP. (a) Overall block diagram. (b) Photograph of an overall experimental setup.

system includes five parts: an SPMSM, a three-phase two-level pulse-width modulation (PWM) inverter, a control board with a TI TMS320F28335 DSP, a magnetic powder brake, and an optical incremental encoder. A single-phase H-bridge diode is used to rectify the grid AC voltage (220 V/60 Hz) that supplies the dc-link voltage (V_{dc}) to the inverter. As depicted in Fig. 3, the two actual phase currents (i_a, i_b) on the stator windings are measured by using two Hall-effect current sensors LTS6-NP via a 12-bit A/D converters. Also, the motor speed is extracted from the position (θ) acquired by an optical incremental encoder E40HB-6-2500-3-N-24 mounted in alignment with the shaft of motor. It is noted that this paper uses the space-vector PWM (SVPWM) technique to supply less harmonic voltage from the three-phase inverter to the SPMSM. The sampling time (T_s) and PWM switching frequency (f_s) are set as 200 μs and 5 kHz [21], [36], respectively, based on the control performance and system efficiency in the simulation and experiment parts.

It is noted that the test-bed uses the Code Composer Studio Development Tools v3.3 (CCSv3.3) software as a code composing tool. To transfer and receive the data between the Host-PC and DSP board, the RealDSP DataMon v2.0 software and the RealDSP-UT are utilized as a hardware management software and an intermediate transfer device, respectively. First, the main program of the control algorithm is composed in the CCSv3.3 environment by using the C code. Then, the compiled file, which is generated by building the main programming project created for the current work, is downloaded into the DSP board by using the RealDSP DataMon software via the RealDSP-UT device. Finally, the real time data for the variables such as the control flags, speed references, and control gains can be established and adjusted online thanks to the intuitive interface of the RealDSP DataMon platform. Fig. 4 shows the implementation flowchart of the proposed NDO-based SMSC algorithm using the C code.

```
void main(void) {
- Disable CPU interrupts and clear all CPU interrupt flags
- Initialize: SCI for data monitoring
              GPIO module
              ADC module
              DAC module
              Sequence Timer module
              PWM module
              Encoder module
- Enable Global realtime interrupt
  interrupt void InterruptFunction(void) {
   - Enable PWM interrupt routine
   - Initialize the parameters
   - Calculate the rotor position (θ) from the encoder signal
   - Measure the phase currents (i_a, i_b)
   - Clark and Park transformations (i_qs, i_ds)
   - Nonlinear disturbance observer (NDO)
   - Proposed NDO-based sliding mode speed controller (v_qs, v_ds)
   - Inverse Park transformation (v_α, v_β)
   - Space Vector PWM update
   }
}
```

FIGURE 4. Implementation flowchart of the proposed NDO-based SMSC algorithm using the C code.

The next subsection presents the good performance of the proposed NDO under load torque step-change and parameter uncertainties by analyzing the comparative results between the proposed NDO (7) and conventional LDO [26].

A. COMPARATIVE RESULTS OF CONVENTIONAL LDO AND PROPOSED NDO UNDER LOAD TORQUE STEP-CHANGE AND PARAMETER UNCERTAINTIES

This subsection examines the performance of the proposed NDO by comparing the outputs of the conventional LDO and proposed NDO in a condition of sequentially combining the change of the rotor speed and load torque disturbance. As shown in (3), the parameter uncertainties and sinusoidal change of unmodeled dynamics are also investigated in this simulation. First, in case of the parameter uncertainties, the stator resistance R_s can naturally vary in the range of $+10\%$ to $+60\%$ from the nominal value due to the temperature changes throughout operation [37]. The stator inductance L_s can be

deviated from its nominal value in the scope of −10% to −30% [7] because of the temperature variations and magnetic saturation caused by the stator currents [14]. Also, the magnetic flux linkage is changed from +10% to −30% of the nominal value due to the temperature changes [37]. Regarding the mechanical parameters, the equivalent rotor inertia (J) and viscous friction coefficient (B) can be significantly distorted because of the external mechanical loads [38]. Synthetically, the parameter uncertainties of the SPMSM in this paper are set as $\Delta J = +80\%\ J$, $\Delta B = +100\%\ B$, $\Delta L_s = -30\%\ L_s$, $\Delta R_s = +60\%\ R_s$, and $\Delta\phi_f = -30\%\ \phi_f$ to inspect the estimation performance of the proposed NDO. Second, in case of the sinusoidal change of unmodeled dynamics, the first unmodeled dynamics (δ_ω) in (3) caused by the acceleration of the rotor speed (ω) are chosen with a sinusoidal value of $10{\cdot}sin(5t)$ by considering the proper upper boundary of magnitude and bandwidth of system [7] to check the steady-state error (SSE) of the proposed NDO. Regarding the rotor materials and motor structure which result in the cogging torque and flux harmonics, the two remaining unmodeled dynamics (δ_q, δ_d) in (3) are designated as the sinusoidal forms [26]. It is noted that the frequency of these sinusoidal forms is selected based on the 6$^{\text{th}}$-order harmonics in comparison with the fundamental frequency [27] and their magnitudes are chosen based on the number of poles and rated current presented in the SPMSM drive. From the parameters listed in Table 1, the δ_q and δ_d are assigned as $30{\cdot}sin(6\omega_o t)$ and $50{\cdot}cos(6\omega_o t)$ [26], respectively, to show the tracking performance of the proposed NDO, where ω_o is the fundamental frequency derived from the electrical angle. In this paper, the parameters for the nonlinear observer gain matrix $L(x_o)$ are selected as $m_1,\ldots,m_6 = (10^3, 1, 10^3, 1, 10^3, 1)$ based on the principle of high gains updated online [21], respectively. In case of the conventional LDO, the linear observer gains are selected based on the internal model principle when ignoring the unmodeled dynamics [39]. In this paper, the linear observer gains L are chosen as $diag(1000, 1000, 1000)$.

Fig. 5 shows the comparative simulation results of the disturbance values estimated by the conventional LDO (i.e., $\hat{d}_{\omega\_Con}$, $\hat{d}_{q\_Con}$, and $\hat{d}_{d\_Con}$) and proposed NDO (i.e., $\hat{d}_{\omega\_Pro}$, $\hat{d}_{q\_Pro}$, and $\hat{d}_{d\_Pro}$). In this figure, the mechanical disturbance ($\hat{d}_{\omega\_Pro}$) observed by the proposed NDO has the faster settling time (15 ms) than that ($\hat{d}_{\omega\_Con}$) by the conventional LDO (30 ms) when the load torque suddenly changes from 1.2 N·m to 2.4 N·m. It is noted that the estimated load torque can be calculated from (3) by ignoring the parameter uncertainties and unmodeled dynamics (i.e., $\hat{T}_L = \hat{d}_\omega/g_3$). In case of the electrical disturbances (d_q) and (d_d), the trajectories of the proposed NDO ($\hat{d}_{q\_Pro}$ and $\hat{d}_{d\_Pro}$) have a shorter delay time (2.1 ms) and smaller SSE than those of the conventional LDO ($\hat{d}_{q\_Con}$ and $\hat{d}_{d\_Con}$) (i.e., longer delay time (4 ms) and larger SSE). In addition, the proposed NDO shows that the speed response has a shorter recovering time (23 ms) and a lower speed overshoot (11 r/min) compared to the conventional LDO (i.e., recovering time: 49 ms and speed overshoot: 26 r/min) when the load torque suddenly changes from 1.2 N·m to 2.4 N·m. Thus, it is clear that the proposed NDO has a better estimation capability than the conventional LDO by showing a faster transient response, smaller SSE, and a faster convergence from choosing the proper nonlinear observer gain matrix $L(x_o)$.

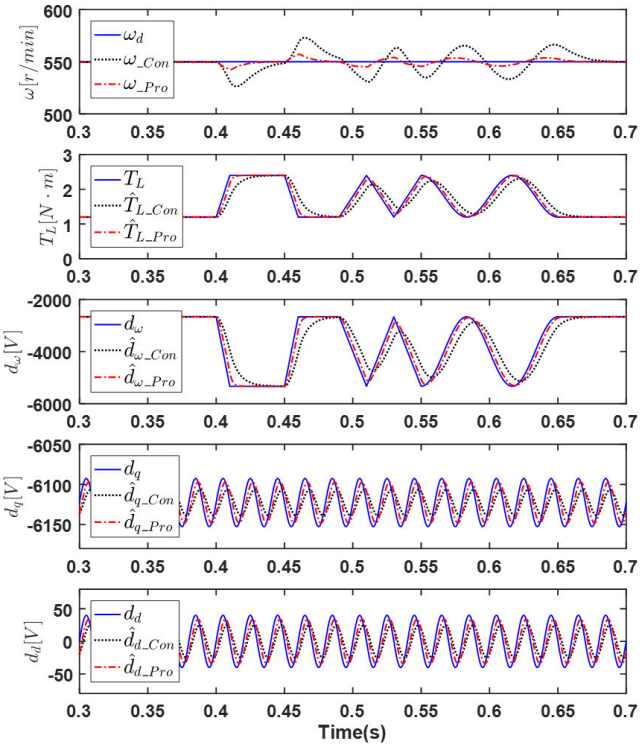

FIGURE 5. Comparative simulation results of the conventional LDO and proposed NDO under load torque step-change and parameter uncertainties.

B. DYNAMIC RESPONSE INVESTIGATION OF CONVENTIONAL LDO-BASED SMSC AND PROPOSED NDO-BASED SMSC

To exhibit the control performance of the proposed NDO-based SMSC and conventional LDO-based SMSC, the two operating conditions are investigated. First, *Condition 1* is chosen to demonstrate the transient performance when the desired speed (ω_d) is suddenly changed from startup (i.e., 0 r/min) to rated speed (i.e., 3000 r/min) at the constant load torque of 1.0 N·m with parameter uncertainties (i.e., $\Delta J = +80\%\ J$, $\Delta B = +100\%\ B$, $\Delta L_s = -30\%\ L_s$, $\Delta R_s = +60\%\ R_s$, and $\Delta\phi_f = -30\%\ \phi_f$). Next, *Condition 2* is selected to verify the fast recovery capability of the proposed NDO-based SMSC when the load torque (T_L) is abruptly changed from 1.2 N·m to 2.4 N·m (rated load torque) at the constant speed command of 1000 r/min with parameter uncertainties (i.e., $\Delta J = +80\%\ J$, $\Delta B = +100\%\ B$, $\Delta L_s = -30\%\ L_s$, $\Delta R_s = +60\%\ R_s$, and $\Delta\phi_f = -30\%\ \phi_f$). In the course of an experiment, it is very difficult to directly change the real system parameters in the SPMSM drives, so the system parameters are modified in the control algorithm

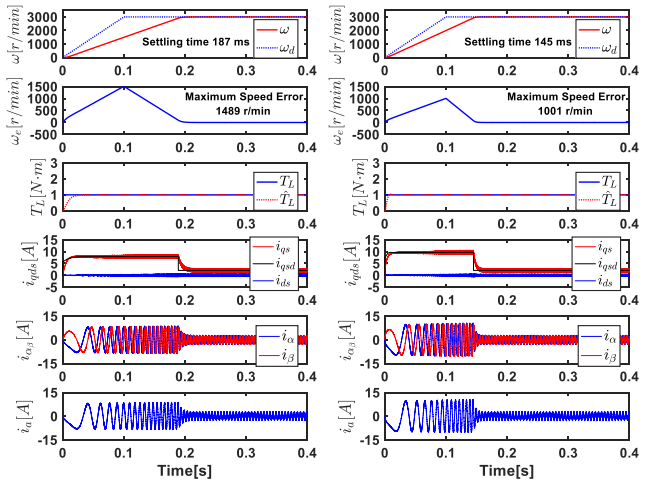

FIGURE 6. Comparative simulation results under *Condition 1* with parameter uncertainties (i.e., $\Delta J = +80\%\ J$, $\Delta B = +100\%\ B$, $\Delta L_S = -30\%\ L_S$, $\Delta R_S = +60\%\ R_S$, and $\Delta\phi_f = -30\%\ \phi_f$). (a) The conventional LDO-based SMSC scheme. (b) The proposed NDO-based SMSC scheme.

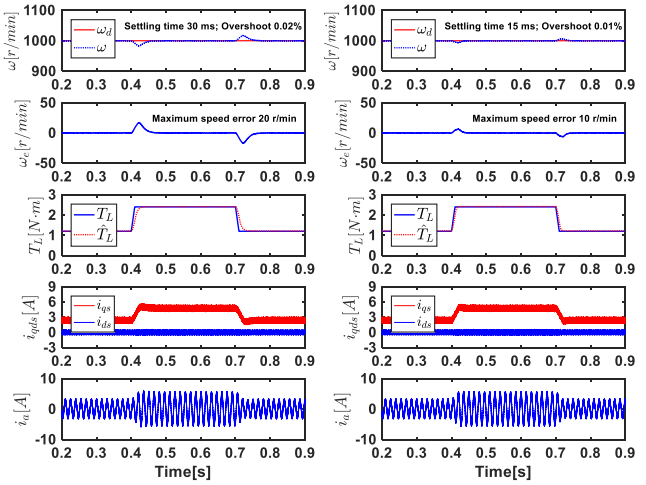

FIGURE 7. Comparative simulation results under Condition 2 with parameter uncertainties (i.e., $\Delta J = +80\%\ J$, $\Delta B = +100\%\ B$, $\Delta L_S = -30\%\ L_S$, $\Delta R_S = +60\%\ R_S$, and $\Delta\phi_f = -30\%\ \phi_f$). (a) The conventional LDO-based SMSC scheme. (b) The proposed NDO-based SMSC scheme.

based on a code composer instead of adjusting the real system parameters [16].

It is noted that the gain (c) contributes to the stabilization of the drive system. If the stabilizing gain (c) is too small, the system will become unstable, while if the gain (c) is too big, the system will be sensitive to the parameter uncertainties. Additionally, the gain values (k_q, k_d, and c) are designed based on the knowledge of the system parameters. If the gain values (k_q and k_d) are too big, the chattering cannot be suppressed, whereas if the gain values (k_q and k_d) are too small, the steady-state error (i.e., speed error) may occur. In this paper, the gain values of the proposed NDO-based SMSC are selected as $k_q = k_d = 1000$ and $c = 100$ based on *Remark 5*.

1) COMPARATIVE SIMULATION RESULTS

Fig. 6(a) and (b) shows the comparative simulation results of the conventional LDO-based SMSC and proposed NDO-based SMSC under *Condition 1* with the parameters uncertainties, respectively. This figure shows the motor speed, speed error, load torque, dq-axis stator currents, and phase-a stator current. It is observed that the proposed NDO-based SMSC in Fig. 6(b) has a much faster speed response (settling time: 145 ms) without overshoot than the conventional LDO-based SMSC response (i.e., settling time: 187 ms) in Fig. 6(a). It means that the proposed scheme can settle faster to steady-state than the conventional scheme.

Fig. 7(a) and (b) presents the comparative simulation results of the conventional LDO-based SMSC and proposed NDO-based SMSC under *Condition 2* with the parameters uncertainties, respectively. Fig. 7(a) shows a poorer speed response (i.e., settling time: 30 ms and speed overshoot: 20 r/min), whereas Fig. 7(b) shows a more stable speed response (settling time: 15 ms) and a smaller speed overshoot (10 r/min) during the transient-state when the load torque profile suddenly changes. Thus, the proposed method exhibits a faster recovering response than the conventional method.

2) COMPARATIVE EXPERIMENTAL RESULTS

Fig. 8(a) and (b) demonstrates the comparative experimental results of the conventional LDO-based SMSC and proposed NDO-based SMSC under *Condition 1* with the parameters uncertainties, respectively. Fig. 8(a) shows that the measured speed (ω) accurately pursues the desired speed (ω_d) in the steady-state with a long settling time (232 ms). Meanwhile, Fig. 8(b) shows that the rotor speed rapidly tracks the desired speed with a shorter settling time (197 ms) and no overshoot in the transient-state. Thus, it can be observed that the proposed NDO-based SMSC has much better tracking performance than the conventional LDO-based SMSC in the speed transient behavior because the tracking errors during the transient are speedily compensated.

Fig. 9(a) and (b) depicts the comparative experimental results of the conventional LDO-based SMSC and proposed NDO-based SMSC under *Condition 2* with the parameters uncertainties, respectively. In this figure, it can be observed that the proposed NDO-based SMSC in Fig. 9(b) reveals a shorter settling time (36 ms) and a smaller speed overshoot (4.5%) of the rotor speed (ω) than the conventional LDO-based SMSC (i.e., settling time: 52 ms and speed overshoot: 8.8%) in Fig. 9(a) during the transient-time. Hence, it can be observed that the speed transient responses for the proposed speed controller are quickly recovered because of its capability to mitigate the abrupt external disturbances. According to Figs. 6−9, Table 2 summarizes the control performance comparison of the conventional LDO-based SMSC scheme and proposed NDO-based SMSC scheme under two

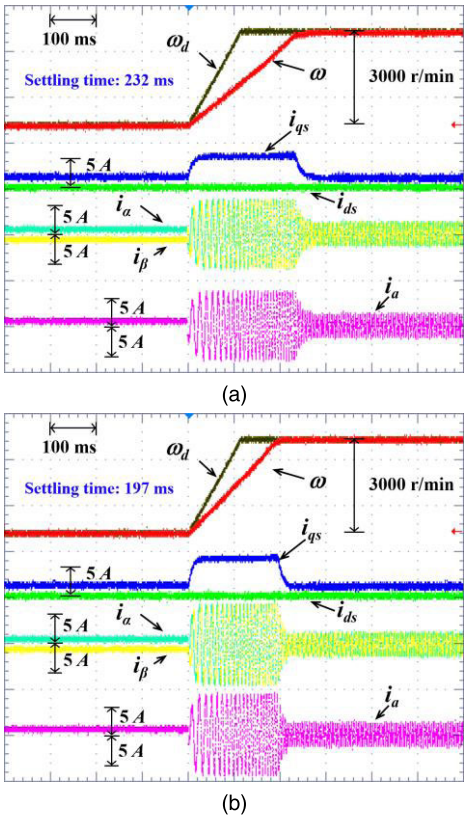

FIGURE 8. Comparative experiment results under Condition 1 with parameter uncertainties (i.e., $\Delta J = +80\%\ J$, $\Delta B = +100\%$ B, $\Delta L_s = -30\%\ L_s$, $\Delta R_s = +60\%\ R_s$, and $\Delta\phi_f = -30\%\ \phi_f$). (a) The conventional LDO-based SMSC scheme. (b) The proposed NDO-based SMSC scheme.

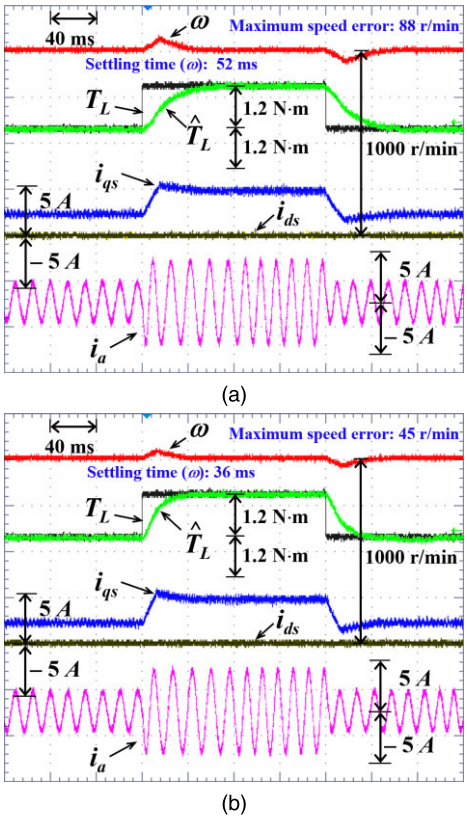

FIGURE 9. Comparative experiment results under Condition 2 with parameter uncertainties (i.e., $\Delta J = +80\%\ J$, $\Delta B = +100\%$ B, $\Delta L_s = -30\%\ L_s$, $\Delta R_s = +60\%\ R_s$, and $\Delta\phi_f = -30\%\ \phi_f$). (a) The conventional LDO-based SMSC scheme. (b) The proposed NDO-based SMSC scheme.

TABLE 2. Control performance comparison of two control schemes under two operating conditions through simulation and experimental results.

Conventional LDO -based SMSC / Proposed NDO-based SMSC		*Condition 1*	*Condition 2*
Comparative Simulation Results	Maximum Speed Error (r/min)	1489 / 1001	20 / 10
	Speed Overshoot (%)	– / –	0.02 / 0.01
	Settling Time (ms)	187 / 145	30 / 15
Comparative Experimental Results	Maximum Speed Error (r/min)	– / –	88 / 45
	Speed Overshoot (%)	0 / 0	8.8 / 4.5
	Settling Time (ms)	232 / 197	52 / 36

operating conditions through the simulation and experimental results.

By analyzing the comparative results listed in Table 2, it is worthwhile to conclude that the proposed NDO-based SMSC has the better disturbance rejection capability and control performance.

VI. CONCLUSION

This paper has presented an NDO-based SMSC scheme with a proper disturbance rejection capability for the SPMSM drives. In ac motor drive applications, the proposed SMSC can achieve the superior control performance such as robustness, fast transient response, and small steady-state error. Additionally, the disturbances can considerably deteriorate the overall control performance of the drive system, so an NDO with a proper disturbance rejection capability is proposed to remarkably improve the trajectory tracking performance of the SMSC designed for the SPMSM drives. The effectiveness of the proposed NDO-based SMSC scheme is validated via the comparative simulation and experimental results on a MATLAB/Simulink software package and a prototype test-bed SPMSM drive with a TI TMS320F28335 DSP when compared to the conventional LDO-based SMSC scheme under load torque disturbances and model parameter uncertainties. Finally, the proposed SMSC can markedly improve its performance such as robust tracking capability, fast dynamic response, and small steady-state error.

REFERENCES

[1] T. D. Do, H. H. Choi, and J.-W. Jung, "θ-D approximation technique for nonlinear optimal speed control design of surface-mounted PMSM drives," *IEEE/ASME Trans. Mechatronics*, vol. 20, no. 4, pp. 1822–1831, Aug. 2015.

[2] Q. Fei, Y. Deng, H. Li, J. Liu, and M. Shao, "Speed ripple minimization of permanent magnet synchronous motor based on model predictive and iterative learning controls," *IEEE Access*, vol. 7, pp. 31791–31800, Mar. 2019.
[3] A. T. Nguyen, M. S. Rafaq, H. H. Choi, and J.-W. Jung, "A model reference adaptive control based speed controller for a surface-mounted permanent magnet synchronous motor drive," *IEEE Trans. Ind. Electron.*, vol. 65, no. 12, pp. 9399–9409, Dec. 2018.
[4] G. Hong, T. Wei, and X. Ding, "Multi-objective optimal design of permanent magnet synchronous motor for high efficiency and high dynamic performance," *IEEE Access*, vol. 6, pp. 23568–23581, Apr. 2018.
[5] Y. Abdel-Rady and I. Mohamed, "A hybrid-type variable-structure instantaneous torque control with a robust adaptive torque observer for a high-performance direct-drive PMSM," *IEEE Trans. Ind. Electron.*, vol. 54, no. 5, pp. 2491–2499, Oct. 2007.
[6] E.-K. Kim, J. Kim, H. T. Nguyen, H. H. Choi, and J.-W. Jung, "Compensation of parameter uncertainty using an adaptive sliding mode control strategy for an interior permanent magnet synchronous motor drive," *IEEE Access*, vol. 7, pp. 11913–11923, Feb. 2019.
[7] Z. Zhou, C. Xia, Y. Yan, Z. Wang, and T. Shi, "Disturbances attenuation of permanent magnet synchronous motor drives using cascaded predictive-integral-resonant controllers," *IEEE Trans. Power Electron.*, vol. 33, no. 2, pp. 1514–1527, Feb. 2018.
[8] W.-H. Chen, J. Yang, L. Guo, and S. Li, "Disturbance-observer-based control and related methods—An overview," *IEEE Trans. Ind. Electron.*, vol. 63, no. 2, pp. 1083–1095, Feb. 2016.
[9] H. Jin and J. Lee, "An RMRAC current regulator for permanent-magnet synchronous motor based on statistical model interpretation," *IEEE Trans. Ind. Electron.*, vol. 56, no. 1, pp. 169–177, Jan. 2009.
[10] Y. Zhang, C. M. Akujuobi, W. H. Ali, C. L. Tolliver, and L.-S. Shieh, "Load disturbance resistance speed controller design for PMSM," *IEEE Trans. Ind. Electron.*, vol. 53, no. 4, pp. 1198–1208, Jun. 2006.
[11] H. Sira-Ramirez, J. Linares-Flores, C. Garcia-Rodriguez, and M. A. Contreras-Ordaz, "On the control of the permanent magnet synchronous motor: An active disturbance rejection control approach," *IEEE Trans. Control Syst. Technol.*, vol. 22, no. 5, pp. 2056–2063, Sep. 2014.
[12] J. L. Flores, C. G. Rodriguez, H. S. Ramirez, and O. D. R. Cardenas, "Robust backstepping tracking controller for low speed PMSM positioning system: Design, analysis, and implementation," *IEEE Trans. Ind. Informat.*, vol. 11, no. 5, pp. 1130–1141, Oct. 2015.
[13] R. Errouissi, M. Ouhrouche, W.-H. Chen, and A. M. Trzynadlowski, "Robust cascaded nonlinear predictive control of a permanent magnet synchronous motor with antiwindup compensator," *IEEE Trans. Ind. Electron.*, vol. 59, no. 8, pp. 3078–3088, Aug. 2012.
[14] Y. A.-R.-I. Mohamed, "Design and implementation of a robust current-control scheme for a PMSM vector drive with a simple adaptive disturbance observer," *IEEE Trans. Ind. Electron.*, vol. 54, no. 4, pp. 1981–1988, Aug. 2007.
[15] A. Mora, A. Orellana, J. Juliet, and R. Cardenas, "Model predictive torque control for torque ripple compensation in variable-speed PMSMs," *IEEE Trans. Ind. Electron.*, vol. 63, no. 7, pp. 4584–4592, Jul. 2016.
[16] N. T.-T. Vu, D.-Y. Yu, H. H. Choi, and J.-W. Jung, "T–S fuzzy-model-based sliding-mode control for surface-mounted permanent-magnet synchronous motors considering uncertainties," *IEEE Trans. Ind. Electron.*, vol. 60, no. 10, pp. 4281–4291, Oct. 2013.
[17] S. Li and H. Gu, "Fuzzy adaptive internal model control schemes for PMSM speed-regulation system," *IEEE Trans. Ind. Informat.*, vol. 8, no. 4, pp. 767–779, Nov. 2012.
[18] S. Li and Z. Liu, "Adaptive speed control for permanent-magnet synchronous motor system with variations of load inertia," *IEEE Trans. Ind. Electron.*, vol. 56, no. 8, pp. 3050–3059, Aug. 2009.
[19] S. Wu and J. Zhang, "A robust adaptive control for permanent magnet synchronous motor subject to parameter uncertainties and input saturations," *J. Elect. Eng. Technol.*, vol. 13, no. 5, pp. 2125–2133, Sep. 2018.
[20] X. Zhang, L. Sun, K. Zhao, and L. Sun, "Nonlinear speed control for PMSM system using sliding-mode control and disturbance compensation techniques," *IEEE Trans. Power Electron.*, vol. 28, no. 3, pp. 1358–1365, Mar. 2013.
[21] S. Li, M. Zhou, and X. Yu, "Design and implementation of terminal sliding mode control method for PMSM speed regulation system," *IEEE Trans. Ind. Informat.*, vol. 9, no. 4, pp. 1879–1891, Nov. 2013.
[22] X. Liu, H. Yu, J. Yu, and L. Zhao, "Combined speed and current terminal sliding mode control with nonlinear disturbance observer for PMSM drive," *IEEE Access*, vol. 6, pp. 29594–29601, May 2018.
[23] B. Xu, X. Shen, W. Ji, G. Shi, J. Xu, and S. Ding, "Adaptive nonsingular terminal sliding model control for permanent magnet synchronous motor based on disturbance observer," *IEEE Access*, vol. 6, pp. 48913–48920, Aug. 2018.
[24] S. Cao, J. Liu, and Y. Yi, "Non-singular terminal sliding mode adaptive control of permanent magnet synchronous motor based on a disturbance observer," *J. Eng.*, vol. 2019, no. 15, pp. 629–634, Mar. 2019.
[25] Y. Deng, J. Wang, H. Li, J. Liu, and D. Tian, "Adaptive sliding mode current control with sliding mode disturbance observer for PMSM drives," *ISA Trans.*, vol. 88, pp. 113–126, May 2019.
[26] J. Yang, W.-H. Chen, S. Li, L. Guo, and Y. Yan, "Disturbance/Uncertainty estimation and attenuation techniques in PMSM Drives—A survey," *IEEE Trans. Ind. Electron.*, vol. 64, no. 4, pp. 3273–3285, Apr. 2017.
[27] W.-H. Chen, "Disturbance observer based control for nonlinear systems," *IEEE/ASME Trans. Mechatronics*, vol. 9, no. 4, pp. 706–710, Dec. 2004.
[28] W.-H. Chen, D. J. Ballance, P. J. Gawthrop, and J. O'Reilly, "A nonlinear disturbance observer for robotic manipulators," *IEEE Trans. Ind. Electron.*, vol. 47, no. 4, pp. 932–938, Aug. 2000.
[29] W. Xu, Y. Jiang, and C. Mu, "Novel composite sliding mode control for PMSM drive system based on disturbance observer," *IEEE Trans. Appl. Supercond.*, vol. 26, no. 7, Oct. 2016, Art. no. 0612905.
[30] Y. Yan, J. Yang, Z. Sun, C. Zhang, S. Li, and H. Yu, "Robust speed regulation for PMSM servo system with multiple sources of disturbances via an augmented disturbance observer," *IEEE/ASME Trans. Mechatronics*, vol. 23, no. 2, pp. 769–780, Apr. 2018.
[31] H. K. Khalil, "High-gain observers in feedback control: Application to permanent magnet synchronous motors," *IEEE Control Syst. Mag.*, vol. 37, no. 3, pp. 25–41, Jun. 2017.
[32] B. L. Walcott and S. H. Zak, "Combined observer-controller synthesis for uncertain dynamical systems with applications," *IEEE Trans. Syst., Man, Cybern.*, vol. 18, no. 1, pp. 88–104, Jan./Feb. 1988.
[33] V. Q. Leu, H.-H. Choi, and J.-W. Jung, "LMI-based sliding mode speed tracking control design for surface-mounted permanent magnet synchronous motors," *J. Electr. Eng. Technol.*, vol. 7, no. 4, pp. 513–523, Jul. 2012.
[34] J. J. E. Slotine and W. Li, *Applied Nonlinear Control*. Englewood Cliffs, NJ, USA: Prentice-Hall, 1991.
[35] H. H. Choi, "LMI-based nonlinear fuzzy observer-controller design for uncertain MIMO nonlinear systems," *IEEE Trans. Fuzzy Syst.*, vol. 15, no. 5, pp. 956–971, Oct. 2007.
[36] Z. Mynar, L. Vesely, and P. Vaclavek, "PMSM model predictive control with field-weakening implementation," *IEEE Trans. Ind. Electron.*, vol. 63, no. 8, pp. 5156–5166, Aug. 2016.
[37] S. J. Underwood and I. Husain, "Online parameter estimation and adaptive control of permanent-magnet synchronous machines," *IEEE Trans. Ind. Electron.*, vol. 57, no. 7, pp. 2435–2443, Jul. 2010.
[38] K. Liu and Z. Q. Zhu, "Mechanical parameter estimation of permanent-magnet synchronous machines with aiding from estimation of rotor PM flux linkage," *IEEE Trans. Ind. Appl.*, vol. 51, no. 4, pp. 3115–3125, Jul./Aug. 2015.
[39] J. Yang, S. Li, and X. Yu, "Sliding-mode control for systems with mismatched uncertainties via a disturbance observer," *IEEE Trans. Ind. Electron.*, vol. 60, no. 1, pp. 160–169, Jan. 2013.

ANH TUAN NGUYEN received the B.S. and M.S. degrees in electrical engineering from the Hanoi University of Science and Technology, Hanoi, Vietnam, in 2010 and 2012, respectively, and the M.S. degree in electrical engineering from the Grenoble Institute of Technology, Joseph Fourier University, Grenoble, France, in 2015. He is currently pursuing the Ph.D. degree with the Division of Electronics and Electrical Engineering, Dongguk University, Seoul, South Korea.

His research interests include electric power systems, control of power converters, and digital signal processor-based electric machine drives.

BILAL ABDUL BASIT received the B.S. degree in electrical engineering from the University of Engineering and Technology, Taxila, Pakistan, in 2014, and the M.S. degree in electrical engineering from the University of Engineering and Technology, Lahore, Pakistan, in 2018. He is currently pursuing the Ph.D. degree with the Division of Electronics and Electrical Engineering, Dongguk University, Seoul, South Korea.

His research interests include digital signal processor-based electric machine drives, distributed generation systems using renewable energy sources, application of artificial intelligence techniques in power systems, and power conversion systems for electric vehicles.

HAN HO CHOI (Member, IEEE) received the B.S. degree in control and instrumentation engineering from Seoul National University, Seoul, South Korea, in 1988, and the M.S. and Ph.D. degrees in electrical engineering from the Korea Advanced Institute of Science and Technology, Daejeon, South Korea, in 1990 and 1994, respectively.

He is currently with the Division of Electronics and Electrical Engineering, Dongguk University, Seoul. His research interest includes control theory and its applications to real-world problems.

JIN-WOO JUNG (Member, IEEE) received the B.S. and M.S. degrees in electrical engineering from Hanyang University, Seoul, South Korea, in 1991 and 1997, respectively, and the Ph.D. degree in electrical and computer engineering from The Ohio State University, Columbus, OH, USA, in 2005.

From 1997 to 2000, he was with the Home Appliance Research Laboratory, LG Electronics Company Ltd., Seoul. From 2005 to 2008, he was a Senior Engineer with the Research and Development Center and the PDP Development Team, Samsung SDI Company Ltd., South Korea. Since 2008, he has been a Professor with the Division of Electronics and Electrical Engineering, Dongguk University, Seoul. His research interests include digital signal processor-based electric machine drives, distributed generation systems using renewable energy sources, and power conversion systems and drives for electric vehicles.